CNRS
Centre National de la Recherche Scientifique

INFN
Istituto Nazionale di Fisica Nucleare

Optimal control theory for the angular control of the full payload for AdV+ Phase II

VIR-0219A-23

Manuel Pinto[1*], Maddalena Mantovani[1], and Julia Casanueva Diaz[1]

[1] *EGO - European Gravitational Observatory*

Issue:

Date: March 10, 2023

VIRGO * A joint CNRS-INFN Project
Via E. Amaldi, I-56021 S. Stefano a Macerata - Cascina (Pisa)
Secretariat: Telephone (39) 050 752 521 * FAX (39) 050 752 550 * Email W3@virgo.infn.it

Contents

1 Introduction **2**

2 State Space modeling of the payload **2**
2.1 Analytical description of the mechanical payload of AdV+ . . . 3
2.2 Diagonalization of the opto-mechanical system . . . 6
2.3 Results of the diagonalization process . . . 8

3 Control regulators design and controllability requirements **9**
3.1 Finite Horizon LQ control . . . 9
3.2 Tuning of Q and R matrices . . . 10
3.3 LQI design for AdV+ Phase II configuration . . . 11
3.4 Preliminary results . . . 12

4 Canonical State Space representation **15**
4.1 Canonical LQI controller . . . 16
4.2 Effect of different tuning of Q_c . . . 16
4.3 Effect of different tuning of R_c . . . 18
4.4 Results . . . 20
4.5 Discussion . . . 23

5 State Estimator design - Kalman Filter **24**
5.1 Simulations and results . . . 26

6 Concluding remarks **29**

References **30**

1 Introduction

In the following document it is presented a formulation of a new control strategy for the angular degrees of freedom of a Fabry-Perot cavity (bottom stage) in the presence of radiation pressure effect for Advanced Virgo+ (AdV+) *Phase II*. The main difference with *Phase I* configuration is the introduction of large terminal masses (Marionetta + Mirror). The different physical dimensions of the two terminal masses and the consequent different momenta of inertia introduce a not negligible asymmetry of the opto-mechanical system which is translated in an impossibility of fully-decoupling all the degrees of freedom. Given this difficulty in diagonalizing the system, the possibility of designing SISO-like controllers (Single Input - Single Output) is left out. Thus, in the present study, a new approach of designing MIMO-like controllers (Multi Input - Multi Output) in time-domain is investigated. Optimal Control Theory will be used in order to design controllers which allow, by the minimization of a specific cost function, to obtain direct closed-loop stability with the optimal phase margin available.
The present document will tackle different topics: starting from the analytical description of the Fabry-Perot cavity, first (i) a State Space formulation of the opto-mechanical system is obtained; then, (ii) the design of a LQR control (namely Linear Quadratic Regulator) with an additional Integrator (i.e. LQI) will be described; eventually, to complete the control loop design architecture, (iii) the design of a state estimator, i.e. Kalman Filter, will be reported, by using realistic data of sensors noise, in order to evaluate robustness and convergence limitation of the filter.
Additionally, two versions of the LQI controller (one in physical and the second in canonical coordinates respectively) will be described, in order to enhance limitation and advantages of the two versions.
All the simulation will be performed in Simulink environment.

2 State Space modeling of the payload

State Space representation is a mathematical description of a physical system which is defined by a matrix notation that relates the system's output response due to an input at any given time. The time evolution of the system variables is subjected to a first-order differential equation.
Such representation is commonly used in control engineering [1], as its mathematical architecture handles well the manipulation of Linear Time Invariant (LTI) systems, and fits most of the controller design tasks, both for SISO and multivariable MIMO systems.
The general description of the State Space representation can be approached considering one of the simplest physical system, that is the harmonic oscillator. The equation of motion of such mechanical system is a second-order differential equation:

$$m\ddot{z}(t) + d\dot{z}(t) + kz(t) = F(t) \tag{2.1}$$

where m is the mass of the system which, subjected to an input force over time $F(t)$, is moving along the z coordinate, dampened by the spring-damper effect k (mechanical stiffness) and d (damping coefficient) respectively.
In order to obtain the State Space representation of such system, we need to linearize the system. This means to rewrite the set of coordinates, which allows to reduce the order of the equation from second to first. This is done by introducing a state vector x which contains the position and its first derivative (velocity) with respect to time of the mass m:

$$x = \begin{Bmatrix} z \\ \dot{z} \end{Bmatrix} \tag{2.2}$$

Given Eq. 2.2, by rewriting Eq. 2.1 with respect to $\ddot{z}$, we can reformulate the equation of motion in matrix form:

$$\begin{Bmatrix} \dot{z} \\ \ddot{z} \end{Bmatrix} = \begin{bmatrix} 0 & 1 \\ -\frac{k}{m} & -\frac{d}{m} \end{bmatrix} \begin{Bmatrix} z \\ \dot{z} \end{Bmatrix} + \begin{bmatrix} 0 \\ \frac{1}{m} \end{bmatrix} F(t) \tag{2.3}$$

Where:

$$\begin{aligned} A &= \begin{bmatrix} 0 & 1 \\ -\frac{k}{m} & -\frac{d}{m} \end{bmatrix} \\ B &= \begin{bmatrix} 0 \\ \frac{1}{m} \end{bmatrix} \\ u &= F(t) \end{aligned} \tag{2.4}$$

In Eq. 2.4, A is called State Matrix and it is a representation of the plant of the system: it is a square matrix and has dimension twice of the number of the degrees of freedom N_{DoF}, i.e. $2N_{DoF}$ x $2N_{DoF}$. It contains all the physical (in this case mechanical) parameters of the described system, such as mechanical stiffness and damping coefficients. It also contains information about the frequency response of the plant, as by computing the eigenvalues of the matrix, the root locus of the principal resonances of the system are obtained.
B is called Input Matrix, and it is a representation of the physical actuator used in order to apply an input to the system. It has dimension $2N_{DoF}$ x N_{Act}, where N_{Act} is the number of actuators available.
u is the input vector that is the physical actuation that is given to the system. In case of a feedback loop, u is the correction coming out from the control loop.
Given this premises, the whole second-order physical system has been reduced to the first-order, and its dynamics is regulated by:

$$\dot{x} = Ax + Bu \tag{2.5}$$

Additionally, we can introduce the measurement equation, which describes the sensors dynamics:

$$y = Cx + Du \tag{2.6}$$

In Eq. 2.6, C is the measurement matrix and represents the modeling of the sensors available. It has dimension N_s x $2N_{DoF}$, where N_s is the number of available probes to measure one physical quantity. D is called Feedthrough matrix, which has dimension N_s x N_{Act}. In case there is no feedforward loop implemented, D matrix is generally equal to zero.

2.1 Analytical description of the mechanical payload of AdV+

Consider the mechanical system described in Fig. 1. The suspended Fabry-Perot cavity is described considering the bottom stage (Marionetta + Mirror) of the full payload. In the present document, the following notation is adopted: the elements are labeled with counter-clockwise numbering. Thus, the Input Marionetta and Input Mirror will be MAR_1 and MIR_2, while End Mirror and End Marionetta will be accordingly MIR_3 and MAR_4. Each element of the system is connected between each other through an equivalent elastic-damping element (either longitudinal or torsional) represented by a stiffness k_* and a damping coefficient d_*. The two mirrors are connected by radiation pressure effect, which can be described by an equivalent optical spring with stiffness k_{OS}. As an approximation, the upper stage above the marionettas is considered to be a fixed reference, i.e. no motion in any degrees of freedom of the reference is allowed.
In order to obtain the State-Space formulation of the double pendulum dynamics, we need to start from the analytical equation of motion of the system.
The general torsional equation of motion is:

$$I_{nm}\frac{\partial^2}{\partial t^2}\theta_{nm} + d_{nm}\frac{\partial}{\partial t}\theta_{nm} + k_{nm}\theta_{nm} = T_{nm}(t) \tag{2.7}$$

Where the subscripts n and m represent the n-th mass of the system and the m-th excited degree of freedom. Accordingly, I_{nm} is the Inertia Momentum of the mass n-th along the m-th direction respectively. θ_{nm} is the angular displacement of the masses for a given torque T_{nm}. The optical spring given by radiation pressure effect couples the laws of motion for the two mirrors [2]. Its equivalent stiffness is given by 2.8:

$$k_{os} = \frac{2PL}{c(1-g_3g_2)}\begin{bmatrix} -g_3 & 1 \\ 1 & -g_2 \end{bmatrix} \tag{2.8}$$

Where P is the power resonating inside the cavity, L is the cavity's length, c is the speed of light and g_* are the cavity parameters defined as:

$$g_n = 1 - \frac{L}{R_n} \tag{2.9}$$

with R_n being the radius of curvature of the n-th mirror.

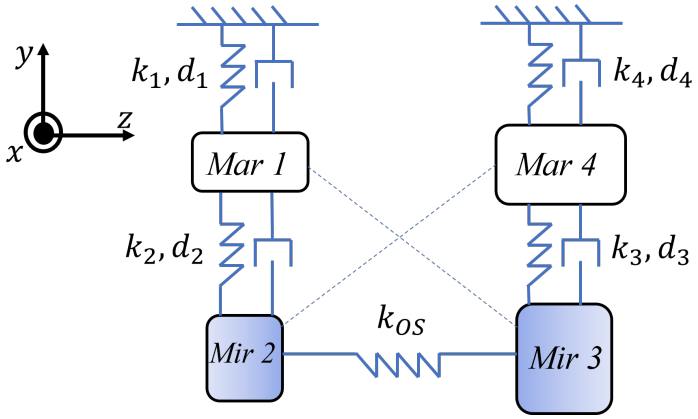

Figure 1: Schematic of the suspended Fabry-Perot cavity (bottom stage).

According to the principle of variation of the Potential Energy, the total stiffness matrix is given by:

$$K_m = \begin{bmatrix} (k_1+k_2) & -k_2 & & \\ -k_2 & k_2 & & \\ & & k_3 & -k_3 \\ & & -k_3 & (k_3+k_4) \end{bmatrix} \tag{2.10}$$

The augmented Optical Stifness matrix, according to 2.8 is given by:

$$K_{OS} = \begin{bmatrix} k_{rpi} & k_p \\ k_p & k_{rpe} \end{bmatrix} \tag{2.11}$$

The total Stiffnes matrix of the opto-mechanical system will be the sum of 2.10 and 2.11, i.e. $K_{tot} = K_m + K_{OS}$. Given this notation, let's consider the TY degree of freedom (Yaw), that is the rotation along the vertical axis. The complete equation of motion is given by:

$$\begin{cases} I_1\ddot{\theta}_1 + k_1\theta_1 + d_1\dot{\theta}_1 - k_2(\theta_2 - \theta_1) - d_2(\dot{\theta}_2 - \dot{\theta}_1) = 0 \\ I_2\ddot{\theta}_2 + k_2(\theta_2 - \theta_1) + d_2(\dot{\theta}_2 - \dot{\theta}_1) + k_{rpi}\theta_2 + k_p\theta_3 = 0 \\ I_3\ddot{\theta}_3 + k_3(\theta_3 - \theta_4) + d_3(\dot{\theta}_3 - \dot{\theta}_4) + k_p\theta_2 + k_{rpe}\theta_3 = 0 \\ I_4\ddot{\theta}_4 + k_4\theta_4 + d_4\dot{\theta}_4 - k_3(\theta_3 - \theta_4) - d_3(\dot{\theta}_3 - \dot{\theta}_4) = 0 \end{cases} \tag{2.12}$$

For the sake of simplicity, in Eq. 2.12, the second index m (DoF excited) has been omitted.
At this point, it is possible to extract the State-Space notation for the full system, by following the same approach described in the previous section. We indeed want to obtain a matrix notation, as done in Eq. 2.3. Thus, by defining the state vector $x^T = [\theta_1\ \dot{\theta}_1\ \theta_2\ \dot{\theta}_2\ \theta_3\ \dot{\theta}_3\ \theta_4\ \dot{\theta}_4]$ we can rewrite the complete law of motion with respect to the second derivative of the angular displacement:

$$\begin{Bmatrix} \dot{\theta}_1 \\ \ddot{\theta}_1 \\ \dot{\theta}_2 \\ \ddot{\theta}_1 \\ \dot{\theta}_3 \\ \ddot{\theta}_1 \\ \dot{\theta}_4 \\ \ddot{\theta}_1 \end{Bmatrix} = \begin{pmatrix} 0 & 1 & 0 & 0 & 0 & 0 & 0 & 0 \\ (-\frac{k_1}{I_1} - \frac{k_2}{I_1}) & (-\frac{d_1}{I_1} - \frac{d_2}{I_1}) & \frac{k_2}{I_1} & \frac{d_2}{I_1} & 0 & 0 & 0 & 0 \\ 0 & 0 & 0 & 1 & 0 & 0 & 0 & 0 \\ \frac{k_2}{I_2} & \frac{d_2}{I_2} & (-\frac{k_2}{I_2} - \frac{k_{rpi}}{I_2}) & -\frac{d_2}{I_2} & -\frac{k_p}{I_2} & 0 & 0 & 0 \\ 0 & 0 & 0 & 0 & 0 & 1 & 0 & 0 \\ 0 & 0 & -\frac{k_p}{I_3} & (-\frac{k_3}{I_3} - \frac{k_{rpe}}{I_3}) & -\frac{d_3}{I_3} & \frac{k_3}{I_3} & \frac{d_3}{I_3} & \\ 0 & 0 & 0 & 0 & 0 & 0 & 0 & 1 \\ 0 & 0 & 0 & 0 & \frac{k_3}{I_4} & \frac{d_3}{I_4} & (-\frac{k_3}{I_4} - \frac{k_4}{I_4}) & (-\frac{d_3}{I_4} - \frac{d_4}{I_4}) \end{pmatrix} \begin{Bmatrix} \theta_1 \\ \dot{\theta}_1 \\ \theta_2 \\ \dot{\theta}_2 \\ \theta_3 \\ \dot{\theta}_3 \\ \theta_4 \\ \dot{\theta}_4 \end{Bmatrix} + \begin{pmatrix} 0 & 0 \\ I_1^{-}1 & 0 \\ 0 & 0 \\ 0 & 0 \\ 0 & 0 \\ 0 & 0 \\ 0 & I_4^{-}1 \end{pmatrix} \begin{Bmatrix} T_{input} \\ T_{end} \end{Bmatrix} \tag{2.13}$$

In Eq. 2.13, the State matrix A, the Input matrix B and the control vector u are explicitly written.
At this point, it is possible to compute the OPEN-LOOP transfer functions of the full coupled system.
The Output VS Input relationship between an arbitrary torque and the correspondent rotation of the masses is given by:

$$\frac{\theta}{T} = C(sII - A)^{-1}B + D \tag{2.14}$$

Where II is the identity matrix of dimensions $2N_{DoF}$ x $2N_{DoF}$.
The Opto-Mechanical parameters of Phase II cofiguration, used for the present study, are reported in Table 1:

Physical quantity	Value	Unit
Circulating Power P	420800	W
Inertia momentum I_{1yy}	3.65	$\frac{Kg \cdot m^2}{rad}$
" I_{2yy}	0.46	$\frac{Kg \cdot m^2}{rad}$
" I_{3yy}	2.34	$\frac{Kg \cdot m^2}{rad}$
" I_{4yy}	6.13	$\frac{Kg \cdot m^2}{rad}$
Damping coefficient d	0.0097	
Mechanical Stiffness k_1	18.94	$\frac{N \cdot rad}{m}$
" k_2	18.94	$\frac{N \cdot rad}{m}$
" k_3	111.78	$\frac{N \cdot rad}{m}$
" k_4	0.3777	$\frac{N \cdot rad}{m}$
RoC Input R_2	1067	m
RoC End R_3	1969	m
Optical Stiffness k_{rpi}	84.032	$\frac{N \cdot rad}{m}$
" k_{rpe}	290.83	$\frac{N \cdot rad}{m}$
" k_p	160.59	$\frac{N \cdot rad}{m}$

Table 1: Opto-Mechanical parameters of Phase II configuration.

Note that in real working condition the value of the damping coefficient can't be calculated but only estimated (or evaluated through experimental measurements). In the present document, it has been used a damping coefficient considering a damping ratio equal to 1% of the critical one, that is $\xi_{opt} = \frac{1}{100}\xi_c$, such that $d = 0.0097$.
According to Eq. 2.14, the opto-mechanical Open-loop transfer functions are reported in Fig.2:

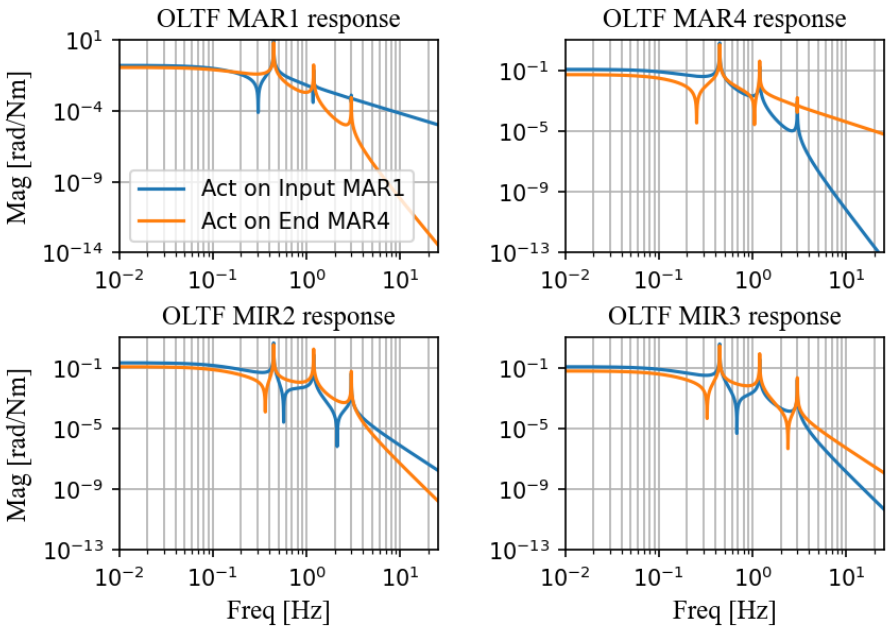

Figure 2: Open-loop transfer functions of the opto-mechanical system, considering a rotation around the TY DoF. In the subplots all the input-output pairings are reported: in blue the masses response due to an arbitrary torque applied on the Input marionetta; in orange, same response due to the actuation on the End marionetta.

In Fig.2 the four subplots represent all the input-output pairings due to the actuations on the two marionettas. In details, blue plots represent the masses response for an applied torque to the Input marionetta, while the orange plots are the ones for the actuation on the End marionetta.
At this point, to decouple the single modes of vibration, the system needs to be diagonalized, in order to switch from the mirror coordinates to the modal coordinates.
The process will shown difficulties to obtain a full diagonal system, mostly due to its asymmetry.
This topic will be object of the next subsection 2.2.

2.2 Diagonalization of the opto-mechanical system

In order to decouple the equations of motion describing the opto-mechanical system, we can use the modal analysis methodology. In our case, we have a system with N_{DoF} degrees of freedom whose equations of motion, in case of forced vibrations, can be generally written in matrix notation:

$$I\ddot{\Theta} + D\dot{\Theta} + K_{tot}\Theta = T(t) \tag{2.15}$$

where I is the Inertia matrix, D is the damping matrix and K_{tot} is the global stiffness matrix (mechanical + optical).
In first approximation, we can consider the mechanical resonances modeled with high Quality factor[1] q that means zero damping, i.e. $D = 0$[2].
To decouple equations of motion in 2.15, we can apply the eigenvalues problems [3][4] which is defined by solving the equation: $det|K_{tot}\text{-}\lambda I|=0$. The aim is to find the Eigenvalues matrix Λ and the Eigenvectors matrix U of

[1]The quality factor of a mechanical resonance goes with the inverse of the damping ratio ξ, as $q = \frac{1}{2\xi}$. We also remember that the damping coefficient d used in the equation of motion can be written as $d = 2\xi\omega I$, where $\omega = 2\pi f$ is the general mechanical angular frequency.

[2]If during the diagonalization process we would want to take into account also of the Damping matrix, we need to consider its value while computing the eigenvectors, that means that D must be diagonalized through $U^T DU$; for reference, see *Frazer, Duncan and Collar* method.

the system. The Eigenvalues matrix is a diagonal matrix which contains the resonance frequencies $\lambda = \omega^2$ of the mechanical system, while the Eigenvectors matrix is a full-square matrix in which each column represents one single mode of vibration.
These two matrices are here defined:

$$\Lambda = \begin{bmatrix} \lambda_1 & & & \\ & \lambda_2 & & \\ & & \lambda_3 & \\ & & & \lambda_4 \end{bmatrix} \tag{2.16}$$

$$U_{iXn} = \begin{bmatrix} y^{i,n} & \varepsilon^{i,n} & \varphi^{i,n} & \zeta^{i,n} \end{bmatrix}$$

where i indicates the i-th eigenvalues, while n is the n-th degree of freedom.
The eigenvalues problem is approached by imposing the ortonormality conditions on the Inertia and on the Stiffness respectively:

$$U^T I U = II; \qquad U^T K_{tot} U = \Lambda \tag{2.17}$$

Ortonormality condition in 2.17 allows to perform a change of coordinates, which means to switch from the physical (mirror bases Θ), to the modal coordinates (mode bases q). This is done by rewriting the equations of motion:

$$\begin{aligned} &\Theta = Uq \\ &I\ddot{\Theta} + K_{tot}\Theta = T(t) \quad \Rightarrow \quad IU\ddot{q} + K_{tot}Uq = T(t) \\ &U^T IU\ddot{q} + U^T K_{tot}Uq = U^T T(t) \\ &\ddot{q} + \Lambda q = U^T T(t) \end{aligned} \tag{2.18}$$

To compute the Eigenvalues and Eigenvectors matrices, we need to solve the eigenvalues problem. For each eigenvalue λ_i we can write the following relationship:

$$det \left| \begin{bmatrix} (k_1+k_2) & -k_2 & & \\ -k_2 & (k_2+k_{rpi}) & k_p & \\ & k_p & (k_3+k_{rpe}) & -k_3 \\ & & -k_3 & (k_3+k_4) \end{bmatrix} - \lambda_i \begin{bmatrix} I_1 & & & \\ & I_2 & & \\ & & I_3 & \\ & & & I_4 \end{bmatrix} \right| = 0 \tag{2.19}$$

$$det \left| \begin{bmatrix} (k_1+k_2)-\lambda_i I_1 & -k_2 & & \\ -k_2 & (k_2+k_{rpi})-\lambda_i I_2 & k_p & \\ & k_p & (k_3+k_{rpe})-\lambda_i I_3 & -k_3 \\ & & -k_3 & (k_3+k_4)-\lambda_i I_4 \end{bmatrix} \right| = 0 \tag{2.20}$$

At this point, from Eq. 2.20, to compute the matrix U, we have to solve the following system of equations for each eigenvalues:

$$\begin{cases} ((k_1+k_2)-\lambda_i I_1)y^{i,n} - k_2\varepsilon^{i,n} = 0 \\ -k_2 y^{i,n} + ((k_2+k_{rpi})-\lambda_i I_2)\varepsilon^{i,n} + k_p\varphi^{i,n} = 0 \\ k_p\varepsilon^{i,n} + ((k_3+k_{rpe})-\lambda_i I_3)\varphi^{i,n} - k_3\zeta^{i,n} = 0 \\ -k_3\varphi^{i,n} + ((k_3+k_4)-\lambda_i I_4)\zeta^{i,n} = 0 \end{cases} \tag{2.21}$$

From the solution of the system of equations in Eq. 2.21, we finally find the Eigenvectors matrix U.

2.3 Results of the diagonalization process

Given the parameters reported in Table 1, the resolution of the system in Eq. 2.21 gave the following eigenvector matrix:

$$U = \begin{bmatrix} -0.4455 & 0.3597 & 0.0859 & 0.0166 \\ -0.3842 & -0.1836 & -0.8404 & -1.12 \\ 0.193 & 0.156 & 0.4143 & -0.423 \\ 0.1402 & 0.2725 & -0.2006 & 0.0228 \end{bmatrix} \tag{2.22}$$

Note that to solve the eigenvalues problems, as mentioned in the previous section, the damping coefficient has been put equal to zero.
According to Eq. 2.18, $U^T T(t)$ gives the mixed actuation that we have to implement to the system in order to excite the different modes of vibration independently. Considering that we have actuation only on the two marionettas, namely $n = 1, 4$, we will have to select only the first and last row in U, by creating the reduced matrix $\tilde{U}$:

$$\tilde{U}^T T(t) = \begin{bmatrix} -0.4455 & 0.1402 \\ 0.3597 & 0.2725 \\ 0.0859 & -0.2006 \\ 0.0166 & 0.0228 \end{bmatrix} T(t) \tag{2.23}$$

In Eq. 2.23, the different pairing of torques to be applied in order to excite the different modes are given.

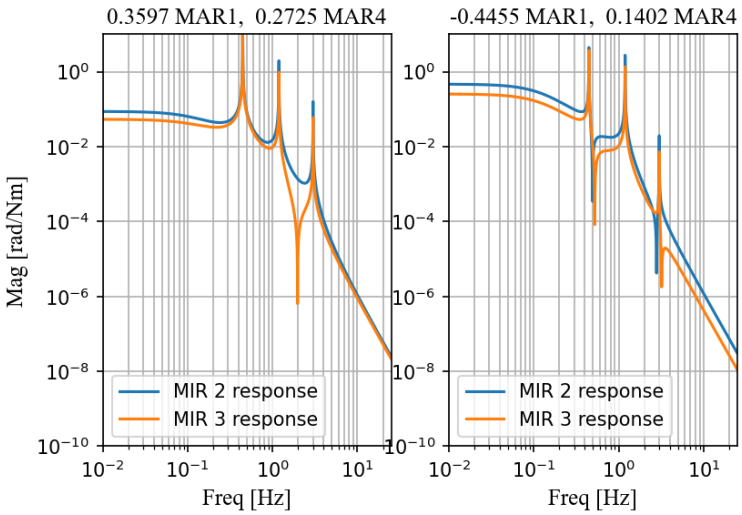

Figure 3: Mirrors response for mixed actuation with torques coming from diagonalization process.

In Fig. 3, response of the mirrors $MIR2$ and $MIR3$ for a mixed actuation on the marionettas is shown. The couple of torques applied are coming from the diagonalization process previously described. As shown, the system can not be fully diagonalized: even if the two mirrors are excited such as they are responding with the same decay at the higher frequency (same roll-off), using both combination of (+) and (-) drivings, all the three modes are excited at the same time. Moreover, some different zero-pole structure is arising between the two TFs.
Results would have been different in case we would have had the possibility to act also on the mirrors instead of only on the marionettas. In such case, we could have exploited the entire Eigenvectors matrix U (and not only the first and last rows), and the possibility to excite the single modes independently would have been achieved.

Given this situation, the possibility to design a SISO-like controller for the different modes of vibrations (in

details, designing one single controller to be splitted to the marionettas) is left out.
In the next sections, it will be explored a new control strategy, based on the design of an optimal MIMO controller by which we will be able to control all the different modes of the system.

3 Control regulators design and controllability requirements

In the previous section the difficulties arising during the diagonalization process of the opto-mechanical system have been analyzed. Given the structural asymmetry, it is not possible to find a couple of eigenvectors, i.e. a couple of torques applied as input to the two marionettas, which allows to excite one resonance mode with respect to another. This implies that the whole system can't be reduced to a "single eigenvalues problem" in which we can control separately the different modes of vibration with a SISO-like control strategy. Instead, it is possible to work with the fully coupled system, by designing two controllers applied separately to the two marionettas.
A general MIMO control scheme is reported as follows:

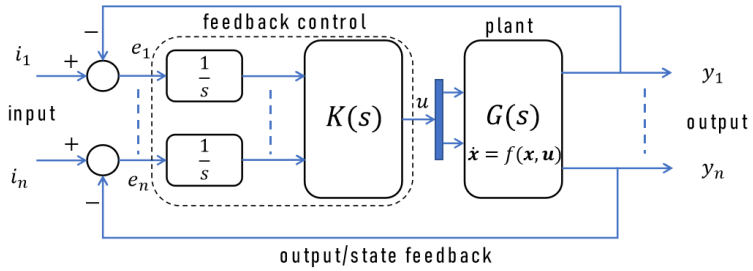

Figure 4: Block scheme of a general MIMO system

Given the plant of the system reported in Figure 4, as a consequence of an input perturbation, according to Eq. 2.14, a rotation of the masses of the double pendula is produced. This rotation is translated into an output vector $y = (y_1, ..., y_n)$, which is used as feedback branch. By comparison with an arbitrary setpoint $i = (i_1, ..., i_n)$, the error signal of the loop $e = (e_1, ..., e_n)$ is produced. Such error signal goes inside the feedback control block which, according to the control strategy implemented, will produce the control vector u which contains the different actuation to be conveniently applied to the available actuators.
In the following section it will be described the Linear Quadratic Integral controller, i.e. LQI. The general mathematical formulation of the LQI controller for linear time invariant (LTI) systems will be reported.

3.1 Finite Horizon LQ control

Consider a second order LTI mechanical system described by $\ddot{x} = f(x, u)$, with initial conditions x_0 at time zero $t_0 = 0$. We can describe the system with the following equations:

$$\dot{x} = Ax + Bu, \quad x(0) = x_0 \tag{3.1}$$

$$J(x_0, u(t)) = \int_0^T x'(\tau)Qx(\tau) + u'(\tau)Ru(\tau)\, d\tau \tag{3.2}$$

where $J(x_0, u(t))$ is defined the *performance index*, dependent by the state and the control action over the time span $[0, T]$. The performance index J represents the cost function to be minimized in order to reach a specific target for the state of the system x, for a given control action u. The cost function J assumes a quadratic form in terms of the state and the control. Given the hypothesis that the system (the state vector) is observable, the Q and R matrices (the penalty matrices for the state and the control, respectively), are squared positive defined, namely $Q \geq 0$, $R \geq 0$.

The general formulation of the LQR control strategy is the following: the objective is to minimize the quadratic cost function:

$$min(J) = \frac{1}{2}\int_0^T x^T Q x + u^T R u \, dt \tag{3.3}$$

which is subjected to:

$$\dot{x} - Ax - Bu = 0, \quad x(0) = x_0 \tag{3.4}$$

The feedback control equation that minimizes the functional J, assumes the form:

$$u = -K_{LQR}(x - x_T) \tag{3.5}$$

where x is the time-dependent state vector, while x_T is an arbitrary set-point.
K_{LQR} is the feedback transfer matrix which contains specific weights which regulates the input to be applied to the available actuators. The value of K_{LQR} is found by solving the first-order differential Riccati equation:

$$A^T P + PA - PBR^{-1}B^T P + Q = -\dot{P} \tag{3.6}$$

$$K_{LQR} = R^{-1}B^T P \tag{3.7}$$

3.2 Tuning of Q and R matrices

In order to achieve an optimal solution and a performant controller (e.g. in terms of rise time, settling time, phase margin ecc..), the weights coefficients within the penalty matrices Q and R, namely the costs on the state and the control, must be carefully chosen.
Given a general state vector containing the several states of the system in the form $x^T = [x_1, x_2, ..., x_n]$ and a general control vector $u^T = [u_1, u_2, ..., u_n]$, we define the penalty matrices as follows:

$$\begin{aligned} Q = &\begin{bmatrix} q_1 & & & \\ & q_2 & & \\ & & \ddots & \\ & & & q_n \end{bmatrix} \\ R = &\begin{bmatrix} r_1 & & & \\ & r_2 & & \\ & & \ddots & \\ & & & r_n \end{bmatrix} \end{aligned} \tag{3.8}$$

Each element on the diagonal of the two matrices represents the cost to be put to each component of the state vector and to each actuator respectively. For what concerns the State penalty matrix Q, the general idea is that the bigger is the chosen weight, the higher will be the cost if the loop doesn't bring the correspondent state to the target set-point. This implies that the several weights will be reasonably big, if we want to guarantee convergence at the steady state, that is if we want x to stabilize quickly and to keep the performance index J small. This means that larger values of the State cost weights will result in larger poles of the Closed loop system so that the dynamics will converge faster to the zero.

Same attention needs to be put regarding the chosen weights for the control penalty matrix R. Big or low costs on the actuation can be chosen depending if we want to design a cheap or expensive controller. One or the other choice will have consequences on the performances (e.g. too high settling time or higher step response, re-injection of noise, loss of sensitivity, ecc..).
Generally speaking, larger R coefficients mean that less control effort is used, so that the poles are generally

lower, resulting in larger values of the state $x(t)$, with poor steady-state convergence.
In order to synthesize the regulator K_{LQR} to stabilize the plant, it is required that the Observability and Controllability conditions are reached.
In details, given the State matrix A, the Input vector B and the measurement vector C, the pair (A, C) must be detectable/observable and the pair (A, B) must be reachable/controllable:

$$Ob = \begin{bmatrix} C \\ CA \\ CA^2 \\ \vdots \\ CA^{n-1} \end{bmatrix} \; ; \; Ctrb = \begin{bmatrix} B & AB & A^2B & \dots & A^{n-1}B \end{bmatrix} \tag{3.9}$$

To fullfill such requirements both of the Ob and $Ctrb$ matrices must be full-rank (non-zero determinant) [1][5].

3.3 LQI design for AdV+ Phase II configuration

So far, the general feedback control equation of the LQR controller has been derived. However, the relation $R^{-1}B^TP$ doesn't always guarantees steady state convergence. In order to reach the zero of the error signal, an integral action is needed. To include the integrator in the feedback loop, we need to reformulate the system equation of motion by augmenting the State matrix and so the State vector [5].
Given the error signal $e_n(t)$ defined, according to the scheme in Figure 4, as:

$$\dot{v_n}(t) = i_n(t) - y_n(t) = e_n(t) \tag{3.10}$$

and the measurements:

$$y = Cx + Nd \tag{3.11}$$

where d is an unmodeled disturbance term, i.e. measurement noise, and C is the measurement (or observation) matrix, the state vectors becomes:

$$\tilde{x} = \begin{Bmatrix} x \\ v \end{Bmatrix} \tag{3.12}$$

Accordingly, the complete State Space equation of motion with the augmented version $\tilde{A}$ of the State matrix A becomes:

$$\begin{Bmatrix} \dot{x} \\ \dot{v} \end{Bmatrix} = \begin{bmatrix} A & 0 \\ -C & 0 \end{bmatrix} \begin{Bmatrix} x \\ v \end{Bmatrix} + \begin{bmatrix} B \\ 0 \end{bmatrix} u \tag{3.13}$$

$$\dot{\tilde{x}} = \tilde{A}\tilde{x} + \tilde{B}u \tag{3.14}$$

Now from Equation 3.14 it is possible to solve the Riccati equation (3.6) in order to obtain the feedback control equation (3.7), with the integral action included, namely:

$$K_{LQI} = R^{-1}\tilde{B}^T\tilde{P} \tag{3.15}$$

The controller has been tuned by choosing the $\tilde{Q}$ penalty weights in order to have high cost on the positions and velocities of the input and end mirrors respectively, namely θ_2, $\dot{\theta_2}$, θ_3 and $\dot{\theta_3}$. High cost has been also put on the integrated error signal, that is the augmenting part of the state vector, v. The actuation cost on R has been put equal to 1.
The present system is composed by four masses which represent the mechanical system's degrees of freedom, which in the present section we indicate with N_{DoF}. With N_s we indicate the number of sensors we have available. Thus, the dimensions of the State Space matrices are reported in Table 2:
Given that we are actuating on the two marionettas separately, the K_{LQI} feedback matrix will contains as many rows as actuation are applied to the system (N_{Act}). In the present case, we have one controller for the

State Space matrix	Dimension
A	$2N_{DoF}$ x $2N_{DoF}$
B	$2N_{DoF}$ x N_{Act}
C	N_s x $2N_{DoF}$
x	$2N_{DoF}$ x 1
v	N_s x 1
$\tilde{A}$	$(2N_{DoF} + N_s)$ x $(2N_{DoF} + N_s)$
$\tilde{B}$	$(2N_{DoF} + N_s)$ x N_{Act}
$\tilde{C}$	N_s x $(2N_{DoF} + N_s)$
$\tilde{x}$	$(2N_{DoF} + N_s)$ x 1
$\tilde{Q}$	$(2N_{DoF} + N_s)$ x $(2N_{DoF} + N_s)$
$\tilde{P}$	$(2N_{DoF} + N_s)$ x $(2N_{DoF} + N_s)$

Table 2: Dimensions of the State Space matrices.

Input Marionetta, and one controller for the End Marionetta. These two controllers will fill the first and the second row respectively.
Dimensions of such matrix will be then: $K_{LQI} = N_{Act}$ x $(2N_{DoF} + N_s)$.
At this point, once Riccati equation has been solved, and the feedback control equation has been computed, to close the loop we define a new State matrix A_{CL}, which takes into account of the feedback matrix:

$$A_{CL} = \tilde{A} - \tilde{B}K_{LQI} \tag{3.16}$$

Given the A_{CL} matrix, it is possible to compute the closed loop gain transfer functions, which gives us information about the stability of the system (e.g. whether it is asymptotically stable or not).
Stability of the system is analyzed by computing the locus of the eigenvalues, to make sure that all the real part of the closed-loop poles are negative (LHP).
This corresponds to apply the Nyquist criterion or to study directly the eigenvalues of the closed-loop state matrix A_{CL}.
Preliminary results of this control strategy implementation will be reported in the subsection 3.4.

3.4 Preliminary results

Preliminary results of the implementation of the LQI controller for the angular degrees of freedom are here presented. In the present study, the case of the TY DoFs is analyzed.
The Closed-loop transfer functions have been evaluated according to 3.16. Results are reported in Figure 5:

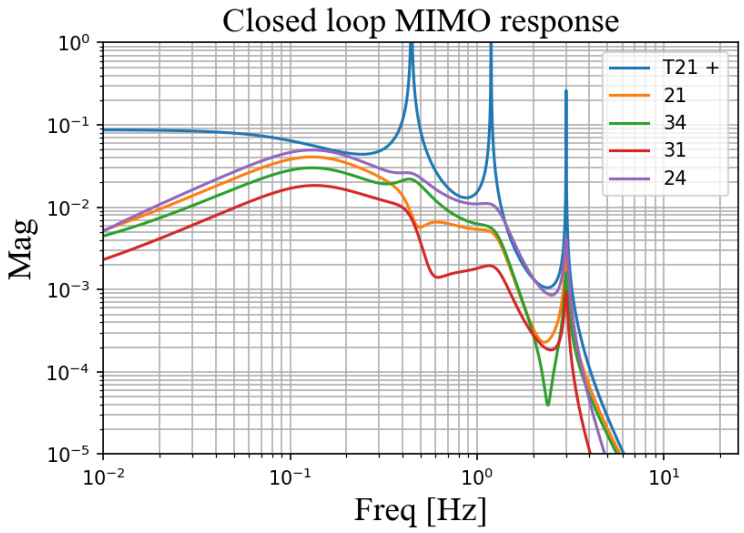

Figure 5: Closed-loop response of the LQI controller for a MIMO system fully coupled

In Figure 5 are reported the different Closed-loop transfer functions (MAR2MIR) of the mechanical system with a LQI feedback control action. In details, the blue plot represents one of the open-loop plant (as reference) of the MAR2MIR response due to the application of a positive torque ratio between the Input marionetta and the End marionetta and the consequent response of the input mirror. In such open loop, the three different modes of vibrations are enhanced.
The other four plots represent the frequency response of the two mirrors for a given torque (under integral control action) to the two marionettas: in details the orange plot represents the MIR2 (input mirror) response for a given actuation to MAR1 (input marionetta); the green plot represents the MIR3 (end mir) for an actuation to MAR4 (end marionetta). The red and purple plots represent the cross-response of the end and input mirrors for an actuation on the input and end marionettas respectively.
Stability of the loop is evaluated computing the eigenvalues of Equation 3.16. Results are reported in Figure 6: as shown, all the real-part of the poles of the Closed-loop system rely on the left half of the complex plane, meaning that the system reaches stability.
One aspect to be noticed, is that with the present control strategy, all the plant unstable poles (mechanical resonances) are damped. However, regarding the high-frequency mode, the one at 3 Hz, there's still some residual oscillation (peaks in the closed-loop).

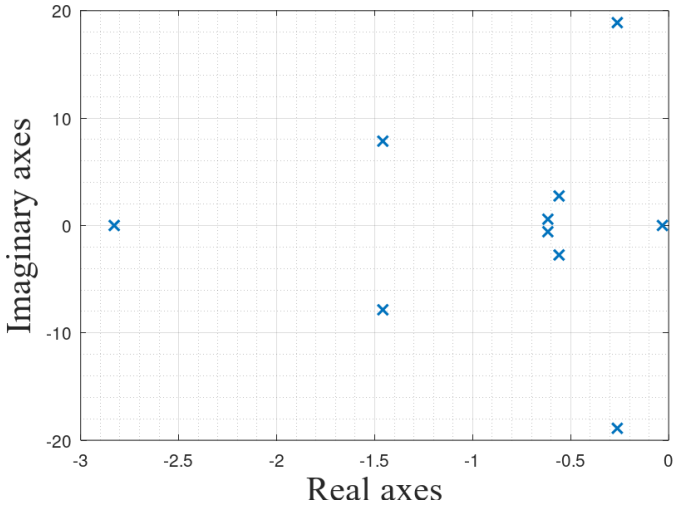

Figure 6: Root locus of the Closed-loop eigenvalues

To perform the time-domain simulations and analysis, MATLAB-Simulink software has been used. In Figure 7 is reported the block scheme representing the feedback control loop: the block in red contains the mechanics of the double pendulum (plant); the green block contains the LQI controller. The control logic implemented is a negative feedback in which the error signal is created as the difference between state x at the time t and an arbitrary setpoint x_T, which has been put to zero. The initial condition is an arbitrary condition as well, set on the angular position of the four masses.

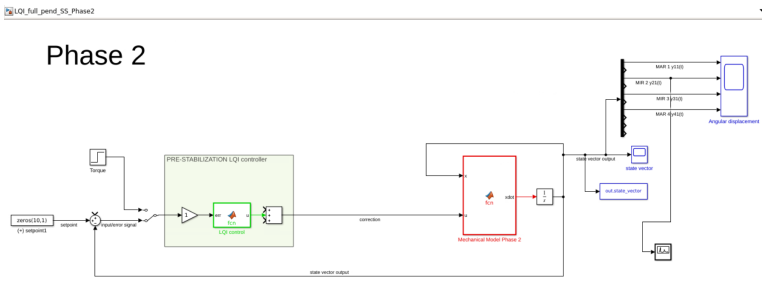

Figure 7: Simulink Block scheme of the optomechanical system

In Figure 8 Simulink simulation results are reported, in details the time-domain response of the angular displacement of the four masses of the system are shown. Performance of the controller can be preliminarily analyzed: the system presents steady-state stability, as the signals reach the zero over a certain amount of time. However, as already reported in the closed-loop transfer function analysis, the system present a residual oscillation of 3 Hz, with an overall settling time of more or less 15 seconds. The settling time could be reduced acting on several aspects: one solution could be to adjust the cost weights on the control penalty matrix $\tilde{R}$. However, this solution will have not negligible consequences on the rise-time of the step response, which will evantually increase, leading to a loss of performace.
One other solution would be to act directly on the controller trying to reduce the 3 Hz oscillation in terms of amplitude. To pursue this task, one difficulty arises since the control design has been performed considering the physical variables of the opto-mechanical system, i.e. angular position and velocities of the masses.
To overcome this issue and to improve the performance of the control strategy, we need to adopt a control design strategy based directly on the modes of vibrations of the system, instead of the physical variables. This

is done by switching to the Canonical State Space representation of the system. Details of this formalism will be reported in Section 4.

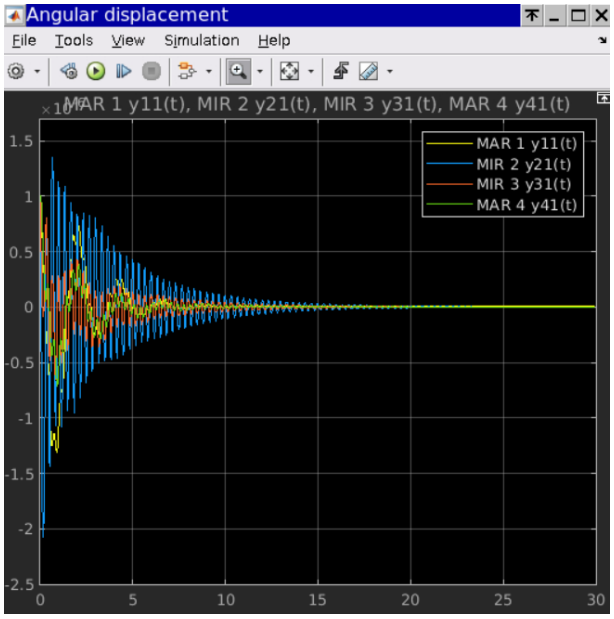

Figure 8: Results of the implementation of the LQI controller. In the plot are reported the time-domain response of the four masses in terms of angular displacement.

4 Canonical State Space representation

The canonical state space representation is obtained performing a state transformation in which through the use of an invertible matrix T we perform a change of coordinates of the mechanical system such that we switch from the physical coordinates to the modal coordinates. The matrix T is a square matrix that allows to rotate the state vector x to x_C:

$$x_c = Tx \tag{4.1}$$

Accordingly, the state matrices of the system become:

$$\begin{aligned} A_c &= TAT^{-1} \\ B_c &= TB \\ C_c &= CT^{-1} \\ D_c &= D \end{aligned} \tag{4.2}$$

With such transformation in 4.2, given a system with complex eigenvalues in the form:

$$\lambda = [\sigma_1 \pm j\omega_1, \sigma_2 \pm j\omega_2, ..., \sigma_n \pm j\omega_n] \tag{4.3}$$

the canonical state matrix assumes the diagonalized form in which all the eigenvalues are separated:

$$A_c = \begin{pmatrix} \begin{matrix}\sigma_1 & \omega_1 \\ -\omega_1 & \sigma_1\end{matrix} & & & \\ & \begin{matrix}\sigma_2 & \omega_1 \\ -\omega_2 & \sigma_2\end{matrix} & & \\ & & \ddots & \\ & & & \begin{matrix}\sigma_n & \omega_n \\ -\omega_n & \sigma_n\end{matrix} \end{pmatrix} \tag{4.4}$$

In the A_c (Eq. 4.4) matrix each block of terms corresponds to a single mode of vibration: thus, during the control design stage, it is possible to put the cost weights of the penalty matrices directly on the relevant modes.

4.1 Canonical LQI controller

The tuning of the LQI controller using the canonical representation has been performed through the same approach described in 3.3.
In order to evaluate the transformation matrix T, MATLAB function *canon* has been used. Thus:

$$T = \begin{pmatrix} -0.1697 & -0.0001 & 1.4472 & 0.0001 & 2.7807 & 0.0000 & -0.3930 & -0.0000 \\ 0.0001 & -0.0090 & -0.0004 & 0.0767 & -0.0004 & 0.1473 & -0.0001 & -0.0208 \\ 0.0003 & -0.1652 & 0.0021 & 0.2036 & 0.0049 & -0.5106 & -0.0006 & 0.6476 \\ 1.2358 & 0.0006 & -1.5233 & -0.0002 & 3.8200 & 0.0006 & -4.8447 & -0.0001 \\ -0.0007 & -1.1911 & 0.0044 & 0.0766 & 0.0022 & -0.3312 & 0.0052 & -1.5153 \\ 3.3386 & 0.0014 & -0.2147 & 0.0000 & 0.9282 & 0.0002 & 4.2473 & 0.0018 \\ -1.2533 & -1.4607 & -0.1810 & -0.2108 & 0.4961 & 0.5795 & 1.2471 & 1.4547 \\ 1.2500 & -1.4613 & 0.1803 & -0.2109 & -0.4970 & 0.5796 & -1.2457 & 1.4550 \end{pmatrix} \tag{4.5}$$

According to Eq. 4.2, the State matrix becomes:

$$A_c = \begin{pmatrix} -0.0068 & 18.8767 & 0 & 0 & 0 & 0 & 0 & 0 \\ -18.8767 & -0.0068 & 0 & 0 & 0 & 0 & 0 & 0 \\ 0 & 0 & -0.0058 & 7.4808 & 0 & 0 & 0 & 0 \\ 0 & 0 & -7.4808 & -0.0058 & 0 & 0 & 0 & 0 \\ 0 & 0 & 0 & 0 & -0.0023 & 2.8030 & 0 & 0 \\ 0 & 0 & 0 & 0 & -2.8030 & -0.0023 & 0 & 0 \\ 0 & 0 & 0 & 0 & 0 & 0 & 0.8559 & 0 \\ 0 & 0 & 0 & 0 & 0 & 0 & 0 & -0.8576 \end{pmatrix} \tag{4.6}$$

In Eq.4.6, the first two terms in row 1 and 2 respectively, represents the 3 Hz eigenmode to be damped. In order to achieve such requierements, in the canonical penalty matrix $\tilde{Q}_c$ related to the state, higher cost has been put to the correspondent elements of the state vector x_c. The same approach has been used for the other vibrational modes. Considering the augmented State matrices, also a consistent high cost has been put to the integrators terms.
Regarding the control penalty matrix R_c, different values have been tried, in order to improve the settling-time VS the rise-time response. However, one choice with respect to the other have to be carefully chosen trying not to have too much high closed loop poles (in absolute values). Indeed, by decreasing the control penalty matrix weights, we will obtain more attenuation, which means that we will move the closed-loop poles further to the left side of the complex plane. Consequences of this action will be to have more attenuation, that is to reduce a lot the settling-time of the state vector at the expenses of the step-response amplitude, which will inevitably increase, with the undesired possibility to saturate the range dynamics of the actuators. One good compromise have been found for R_c to assume unitary values:

$$R_c = \begin{bmatrix} 1 & 0 \\ 0 & 1 \end{bmatrix} \tag{4.7}$$

The final control matrix equation $K_{LQIcanon}$, assumes the following values:

$$K_{LQIcanon} = \begin{pmatrix} -208.2857 & -414.2250 & -7.3965 & 27.6099 & -11.5461 & 8.8472 & -26.0160 & 3.0059 & -16.2106 & -6.1005 \\ -369.8960 & -492.3552 & 43.4128 & -56.7643 & -19.2783 & 5.3229 & 22.1781 & -3.3882 & 6.1005 & -16.2106 \end{pmatrix} \tag{4.8}$$

As for the physical coordinates example, the Closed-loop response has been evaluated, by computing the Closed-loop State matrix:

$$\tilde{A}_{CLcanon} = \tilde{A}_c - \tilde{B}_c K_{LQIcanon} \tag{4.9}$$

4.2 Effect of different tuning of Q_c

As explained in the previous sections, during the controller design stage, several parameters can be tuned in order to achieve more closed-loop attenuation. Those parameters are the cost weights of the Q_c and the R_c matrices. Regarding the state penalty matrix, a global increase of the cost weights allows a more attenuation on the Closed-loop response. In Figure 9 comparison of the four Closed-loop transfer functions (MAR2MIR responses) with different values of the cost weights of Q_c is reported.
In details, on the top-left, subplot of the Input mirror due to the actuation on the Input marionetta is reported. Accordingly, on the top-right is reported the response of the End mirror due to the actuation on the End Marionetta; in the two bottom plot, instead, the cross-response of the End and Input mirrors due to the actuation

on Input and End marionetta respectively is given.
The whole penalty matrix has been multiplied by a global factor of respectively 1 (orange plot), 3 (blue plot) and 5 (green plot) of the originally chosen parameters.
A more strict fine tuning could be done by increasing specifically the weights related to the single mode that we want to attenuate.

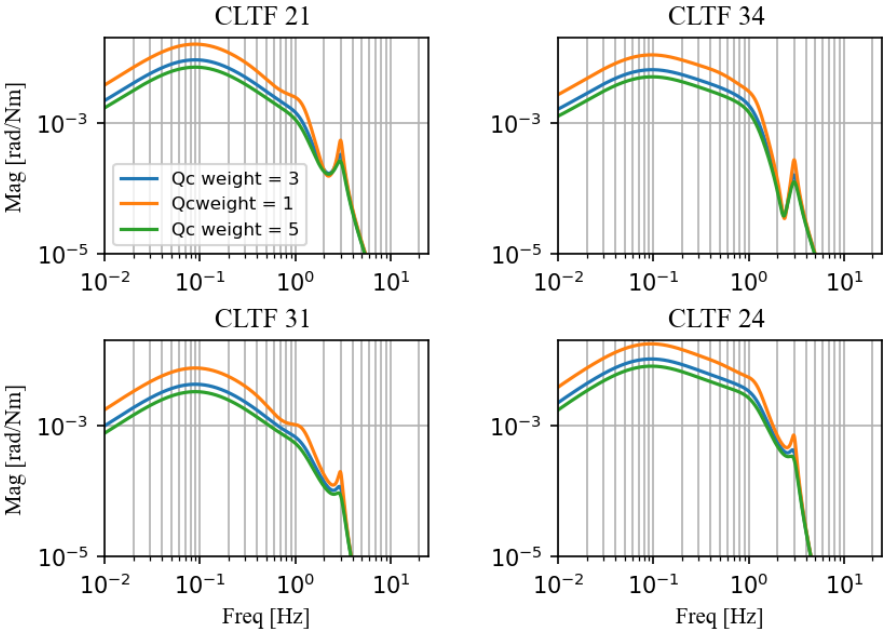

Figure 9: CLTF comparison VS variation of State penalty matrix Q_c

Each tuning choice has consequences to the closed-loop eigenvalues which will eventually increase accordingly to the increase of the costs weights.
In figure 10 is reported the plot of the root locus of the Closed-loop poles in the complex plane, with respect to the chosen tuning parameters.
In order to have sufficient attenuation of the 3 Hz HF mode, a good trade-off has been found by using the global weight of the Q_c equal to 3.

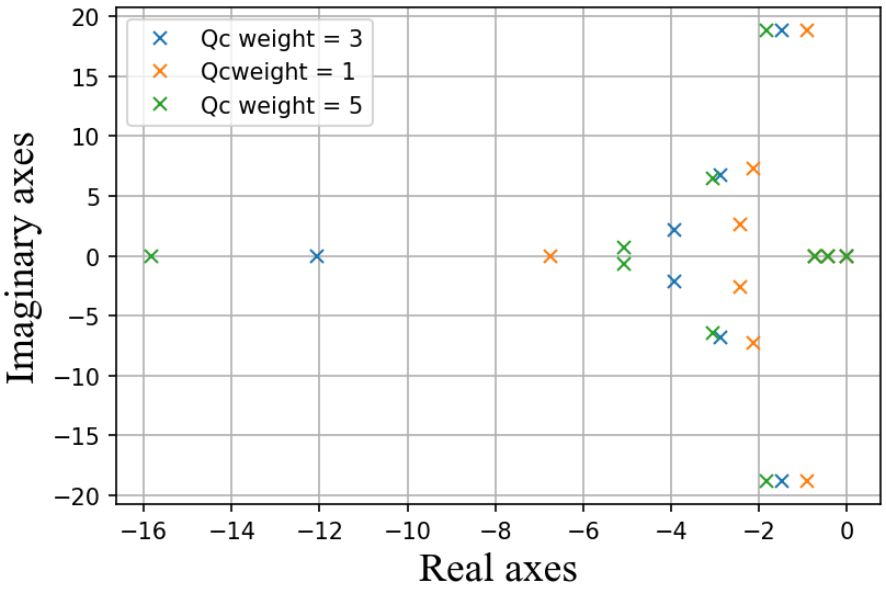

Figure 10: Root locus of the Closed-loop eigenvalues VS different values of State penalty matrix Q_c

4.3 Effect of different tuning of R_c

The same approach can be used also for the tuning of the diagonal elements of the control penalty matrix R_c. This matrix is strictly correlated to the effort that we want to spend to obtain a specific performance of the control actuation.
Given that each diagonal element of the 2X2 R_c matrix corresponds to the actuation on the Input marionetta (MAR1) and End marionetta (MAR4) respectively, by adjusting the weights we can push more or less in the two actuators separately.
In figure 11 is reported the comparison of the MAR2MIR Closed-loop response with respect to different values of the R_c penalty matrix.
Different values of the control penalty matrix used for this study are the following:

$$R_{c1} = \begin{bmatrix} 1 & 0 \\ 0 & 1 \end{bmatrix}; \quad R_{c2} = \begin{bmatrix} 0.1 & 0 \\ 0 & 0.1 \end{bmatrix}; \quad R_{c3} = \begin{bmatrix} 1 & 0 \\ 0 & 0.5 \end{bmatrix} \tag{4.10}$$

As shown, the effect of the tuning is clear: using a reduction of a factor 10, with respect to the unitary values (R_{c1}) of the cost weights causes a global improvement of attenuation of a factor 3, visible in all the four responses (orange plots of Fig. 11).
If we instead change the cost weights only on one actuator, as done in for example in R_{c3}, in which we increase the cost effort on the End marionetta of a factor 2, we obtain a global attenuation of the response of both mirrors of about a factor 1.2, visible on the transfer functions of the mirrors (MIR2 and MIR3) due to the actuation on the End marionetta (MAR4), see green traces on the top right and bottom right subplots.

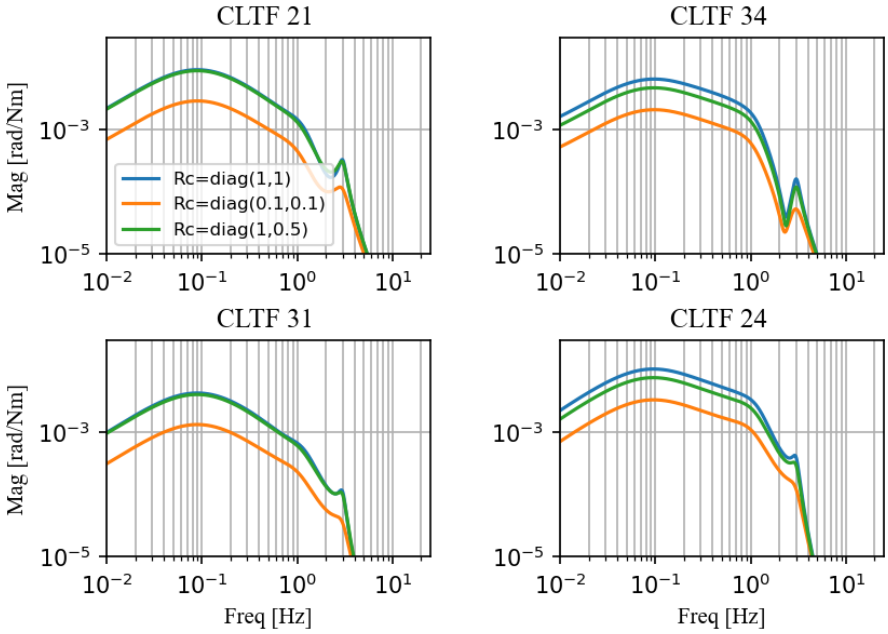

Figure 11: CLTF comparison VS variation of Control penalty matrix R_c

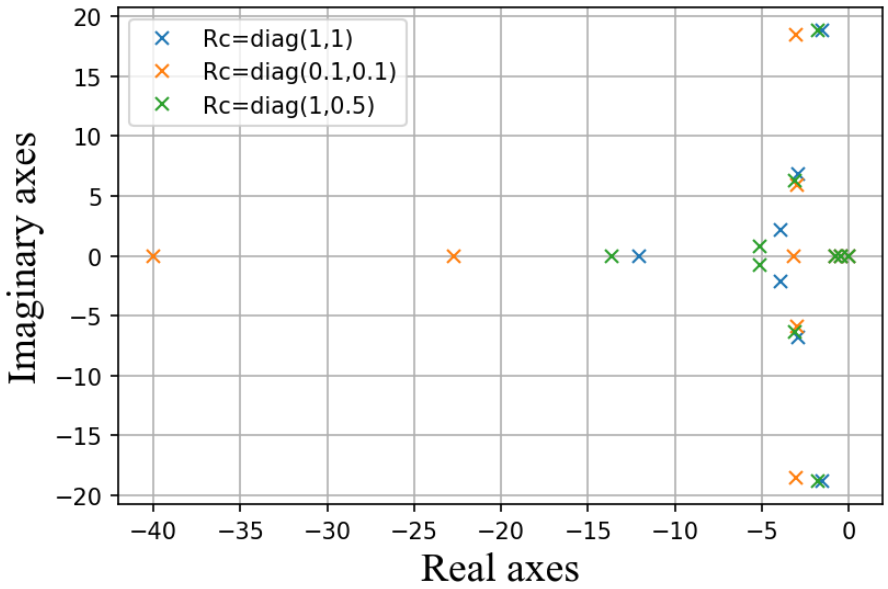

Figure 12: Root locus of the Closed-loop eigenvalues VS different values of Control penalty matrix R_c

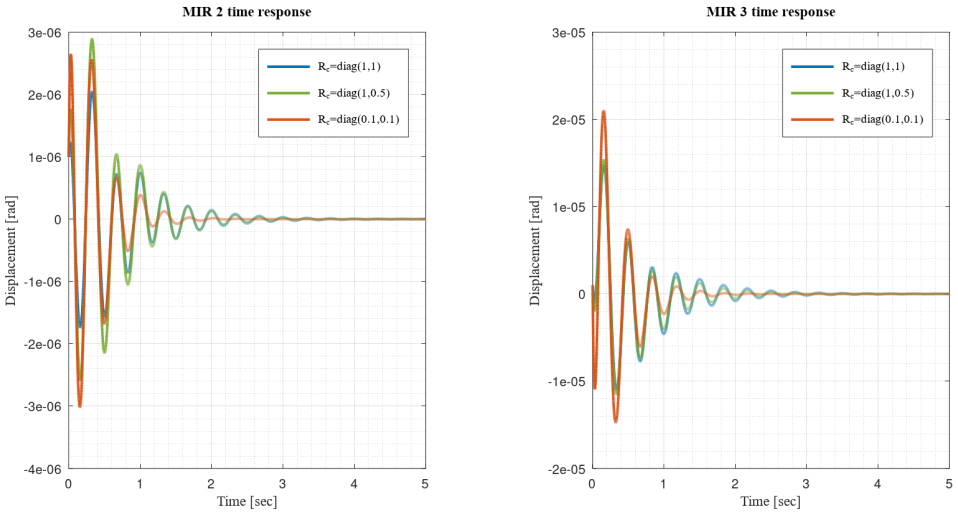

Figure 13: Mirrors time response VS different values of the Control penalty matrix R_c

Results of the implementation of the controller of Eq. 4.8 will be reported in next subsection.

4.4 Results

Results of the implemented strategy are here reported. In Fig. 14 are plotted the Closed-loop gain transfer functions obtained through the Canonical formulation. Such formulation allows to tune the controller by acting directly on the modes that we want to control. As shown, with respect to the previous control example, in the present case it was possible to improve the global attenuation, especially at the 3 Hz mode.

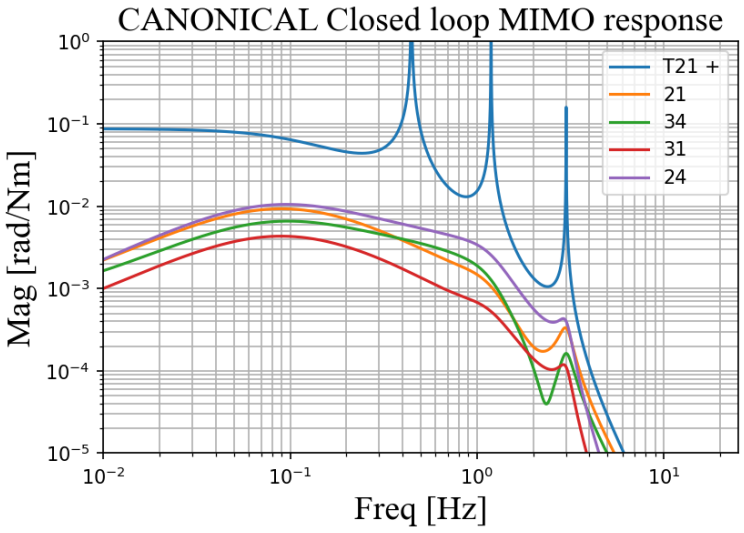

Figure 14: Closed-loop response of the LQI controller for the canonical MIMO system.

Time response of the four masses are reported in Fig. 15.

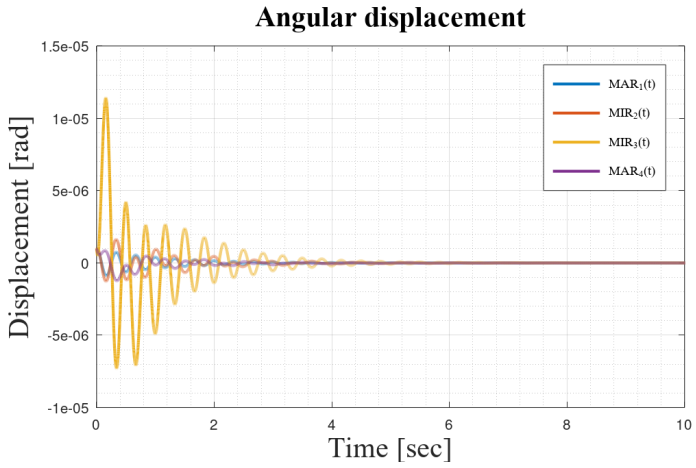

Figure 15: Time response of the angular displacement of the 4 four masses

Performance of the controller can be also evaluated by analyzing the Open-Loop transfer functions of the system. In Fig. 16, Bode plot of the mirrors transfer functions due to the control actions implemented are shown (Input mirror in orange, End mirror in green, Plant MAR2MIR input for reference in blue). Due to the structures of the plant, like zeros, multiple 0 dB crossing are present, however the bandwidth of the loop is defined by the last one. The UGF of the loop, thus, is set beyond the last resonance mode, at around 3.4 Hz.
To be noticed that the design of an optimal control as the LQI, allows to obtain a control loop with theoretically infinite Gain-margin, and at least 60 deg of Phase-margin.
This is verified also in the present case: indeed, at the UGF (3.4 Hz) corresponds a phase of 65.3 deg. As shown in the plot, no decay of the phase at the higher frequencies is present, meaning that the system will be unconditionally stable for every high-gain applied to the loop.

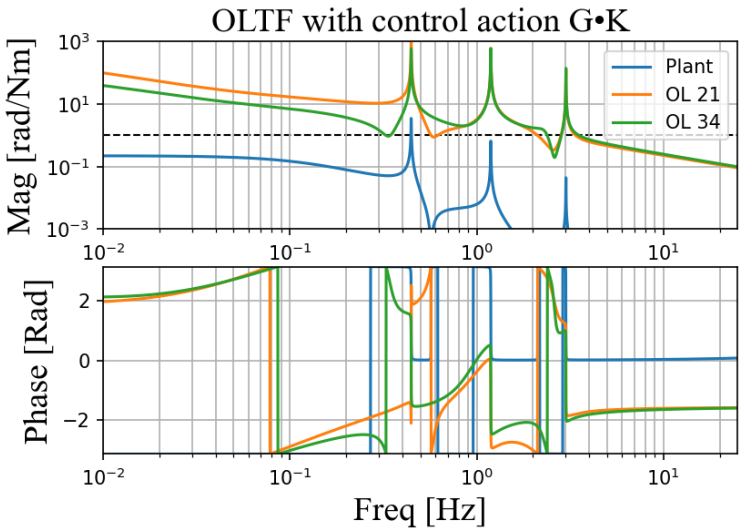

Figure 16: Open-Loop transfer functions of the system with control action.

However, in reality, this will not be plausible since we have to deal with hardware limitations like delay, actuators saturation, or sensor noise reintroduction.
This could be preliminary solved by defining a cut-off frequency by which we set the bandwidth limits. By

implementing for example an additional roll-off filter, we can achieve the requirement of reducing the noise reintroduction. The cut-off frequency will have to be chosen in order not to loose too much of the already available phase. A low-pass filter at 25 Hz fills such requirement.
The adjusted Open-Loop transfer functions with the additional roll-off compensator are shown in the Bode plot of Fig. 17.

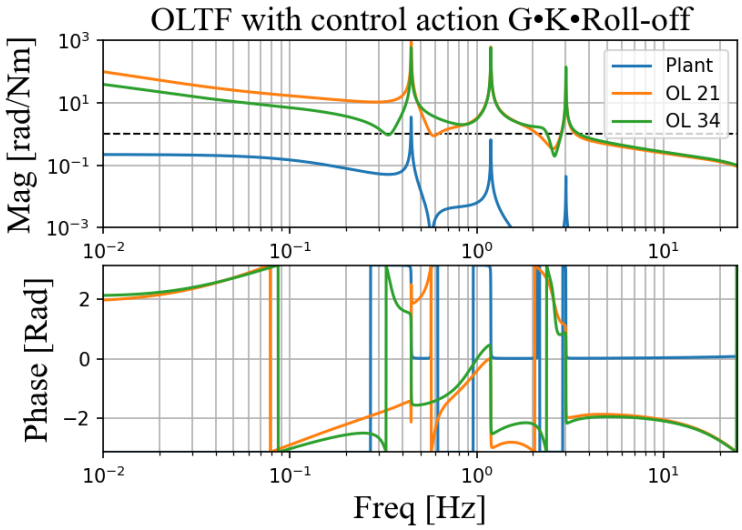

Figure 17: Open-Loop transfer functions of the system with additional Roll-off compensation.

This final compensation allows to obtain a Gain-margin of an additional factor 10, within which the system will be stable. From this value, the system will become unstable, that means it will go under high frequency oscillations.
This eventuality is shown in Fig. 18, in which an increase of gain of a factor 10 has been applied, together with the implementation of the roll-off filter at 25 Hz. As shown, and as expected by the Open-loop plot, the system doesn't converge anymore to the steady state, but diverges by oscillating exactly at 25 Hz, which is the chosen bandwidth upper limit.

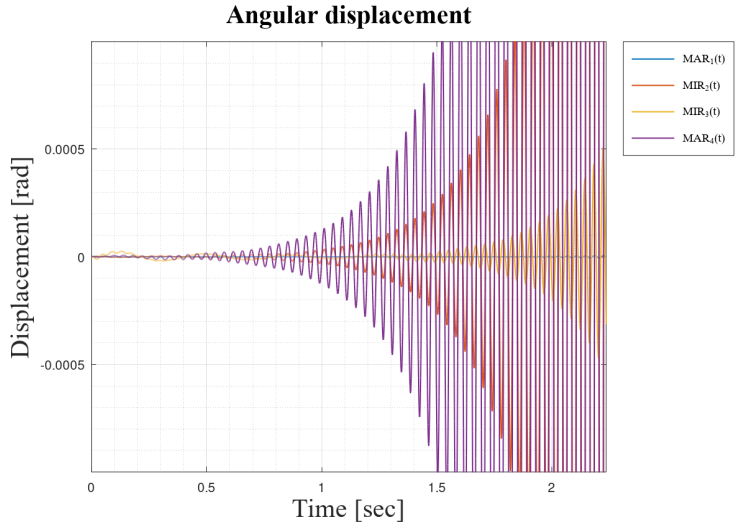

Figure 18: High frequency loop oscillations. Loop gain has been increased by a factor 10.

A final optimization of the control loop, consists in choosing the loop gain in order to have the UGF at the maximum of the Phase: increasing the gain of a factor 2 will move the Unity Gain Frequency up to 5 Hz, with a correspondent Phase-margin between 68 and 72 deg.

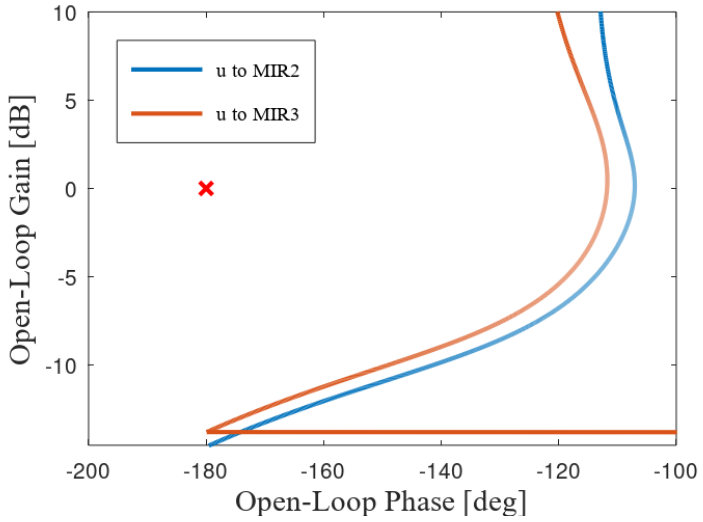

Figure 19: Nichols Chart of the final optimized control: an additional factor 2 has been applied to the loop in order to increase the UGF to 5 Hz. Robustness is well obtained, as the loop still has a factor 5 of Gain-Margin, with a Phase-margin between 68 and 72 deg.

4.5 Discussion

So far, the design of an optimal control filter for stabilizing a coupled opto-mechanical system has been presented. By using the LQI approach, a final controller with bandwidth up to 25 Hz and Phase-margin of at least 60 deg has been obtained.
However, in real working conditions, when designing control filters, we are interested not only in stabilizing the plant, but also in optimizing the low-frequency and the high-frequency regions of the loop. The necessity of improving such regions are due to the requirements of reducing the overall rms of the system and to reduce the re-introduction of sensor noise.
These two goals are achieved by using dedicated structures in the control filters such as Lag Filters (aka Boost Filters), that allow two gain more in the low-frequency region, and consequently to reduce the residual motion of the system.
For what concerns the high-frequency region, the usual structures implemented fall into the category of the Roll-off filters, which are basically Low-Pass filters that allows to reduce the noise re-introduction, cutting the OLTF (slope of the transfer function more steep) above a certain frequency. However, every introduced Roll-off structure, even if it allows to cut-off the noise, on the other hand it will involve a loss of Phase-margin, which will lead eventually to a reduction of the loop bandwidth.
Since we want to reduce the noise re-introduction generally above 10 Hz, this will inevitably cause a huge constraint on the controllability of the higher resonance mode at 3 Hz. We need indeed to find a trade-off between the possibility to have the loop bandwidth ahead of such mode, and to roll-off efficiently the higher frequencies.

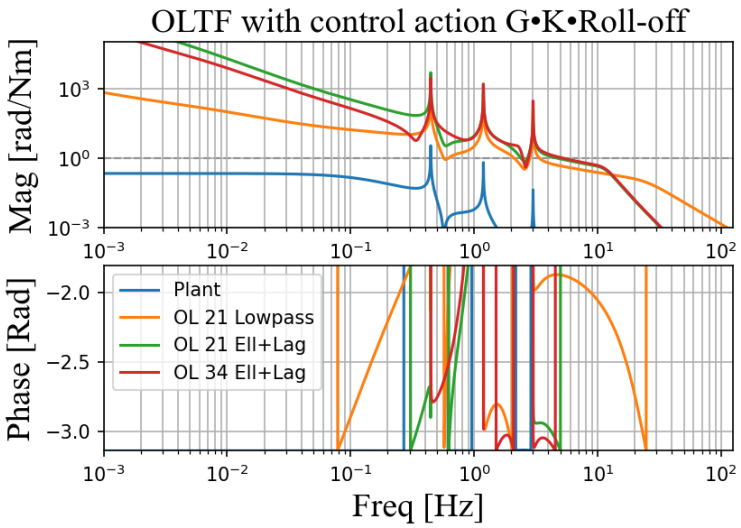

Figure 20: OLTF with Boost and Roll-off actions.

As shown in Fig. 20, cutting the noise ahead 10 Hz with the use of an elliptic filter, will determine a consistent reduction of the Phase-margin of the loop from 68 to around 25 deg. Consequently, the Gain-margin will be very limited.
One solution to increase the overall range of stability margins, with the same rate of roll-off, would be to put the bandwidth of the loop before the last resonance mode. This choice will imply however to left out the possibility to control the 3 Hz mode.

5 State Estimator design - Kalman Filter

So far, we have shown the design principles of a MIMO optimal controller for the angular DoFs of an asymmetric coupled opto-mechanical system. The minimization of the cost function J allowed to achieve the maximum phase margin and bandwidth of the loop, which allows to control all the unstable poles of the system.
However, the implementation of such controller is based on the hypothesis that we are observing the full system, i.e. we are using a full state-feedback loop instead of an output-feedback loop. This means that in order to derive the control law, we are using all the state variables coming out from the state vector, instead of the only available measurement.
In real working conditions, however, we don't have access to the whole variables of the state vector x (e.g. velocities): we have few sensors available which observe only specific portions of the system and produce a signal y. Such signals, provide only a limited knowledge about the system. Additionally, the acquired measurement are generally corrupted by sensors noise and also the process dynamic is affected by some modeling uncertainty. The presence of all these external disturbances contributes to the system to move inevitably away from the setpoint. Under these circumstances, we need a tool which allows to estimate the values of the non-measured variables and to filter out the undesired disturbances.
The Kalman filter allows an estimation $\hat{x}$ of the system state x by performing an optimal blending of the information coming from the given theoretical model and the available measurements.
Such estimate is obtained through a linear combination of the two equation describing the process dynamics and the sensor dynamics, both affected by noises.
The whole technique based on the use of an optimal compensator (LQI) and an optimal estimator (Kalman filter) is called LQIG: Linear Quadratic Integral Gaussian controller.
The Kalman filter problem can be formulated as follows [6]. Let's consider the system of equations:

$$\begin{cases} \dot{x} = Ax + n_d \\ y = Cx + n_s \end{cases} \tag{5.1}$$

where n_d and n_s represent the model error (presence of an extra signal coming from some non-modeled part of the process, as for example seismic noise) and the sensor noise respectively.
The optimal representation of the estimated state $\hat{x}$ we can provide for x is obtained through:

$$\dot{\hat{x}} - A\hat{x} - K_E(y - C\hat{x}) \tag{5.2}$$

where K_E is a gain matrix that mixes the two equations producing the aforementioned blending. The values of such matrix is an indication of the ratio between the process error and the measurement noise and defines whether the Kalman filter should follow closer the process dynamics evolution or the measurements acquired: smaller values of K_E implies that the modeling of the system dominates in the estimation process; on the contrary, high values of the matrix means that the measurement is leading the estimation.
Considering that $\dot{x} - Ax - n_m = 0$ we can subtract it to Eq. 5.2 such that:

$$\dot{\hat{x}} - A\hat{x} - K_E(y - C\hat{x}) - (\dot{x} - Ax - n_d = 0) \tag{5.3}$$

By solving Eq. 5.3 and considering the measurment vector $y = Cx + n_s$ we obtain:

$$\dot{\hat{x}} - \dot{x} - A(\hat{x} - x) + K_E C(\hat{x} - x) - K_E n_s + n_d \tag{5.4}$$

If we introduce the quantities representing the error dynamics:

$$\begin{cases} \dot{\hat{x}} - \dot{x} = \dot{e} \\ \hat{x} - x = e \end{cases} \tag{5.5}$$

we finally obtain the complete estimation error dynamics:

$$\dot{e} = (A - K_E C)e + K_E n_s - n_d \tag{5.6}$$

In order to have an optimal estimation of the state vector $\hat{x}$ we want to minimize the error e, which means to minimize its square modulus, i.e. $L(t) = E\{e^T e\}$. Equivalently we want to minimize the trace of the covariance matrix L, thus:

$$min \int_0^T E\{e^T e\}\, dt \; = min \int_0^T Tr(L)\, dt \tag{5.7}$$

Without getting into the analytical details of this problem, to solve Eq. 5.7, we have to solve a 1st order differential equation, i.e. Joseph's equation, which describes the evolution of the covariance matrix:

$$\dot{L} = LA^T - LC^T K_E^T + AL - K_E CL + K_E R_s K_E^T + R_d \tag{5.8}$$

By solving Eq. 5.8, we finally compute the optimal Kalman gain matrix:

$$K_E = LC^T R_s^{-1} \tag{5.9}$$

In the presence of an additional control action, as e.g. LQR/LQI, the previous formulation will take into account also the feedback controller, by using the estimated state $\hat{x}$ as feedback branch:

$$\dot{\hat{x}} - A\hat{x} - Bu - K_E(y - C\hat{x}) \tag{5.10}$$

with:

$$\dot{x} - Ax - Bu - n_d = 0 \tag{5.11}$$

so that the final control equation[3] becomes:

$$u = -K_{LQI}(\hat{x} - x_T) \implies u = -R^{-1}B^T P(\hat{x} - x_T) \tag{5.12}$$

[3] We remember that P is the matrix coming from the resolution of the Riccati equation for the LQ problem.

The whole control loop together with the estimation block assumes the scheme reported in Fig.21:

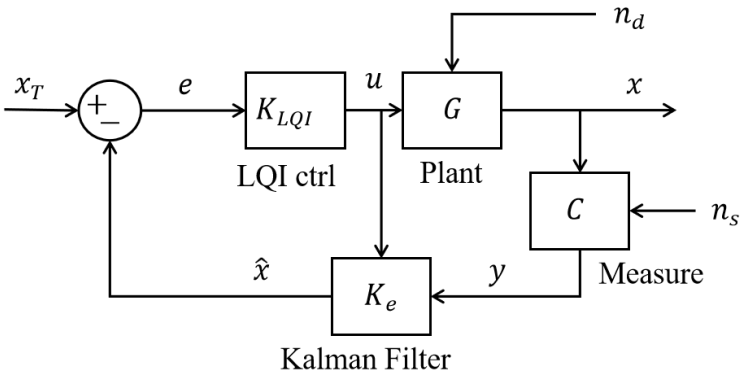

Figure 21: Kalman Filter block scheme.

As shown, the Kalman block is fed with the control action u and the measurements coming from the sensors block C. The output of the Estimator block, i.e. the full estimated state vector $\hat{x}$, is sent to the feedback branch and it is used to compute the control action, which closes the loop.

In the next subsection, results of the implementation of the Kalman filter in Simulink environment will be reported.

5.1 Simulations and results

Results of the implementation of the Kalman filter for the control problem of Eq. 4.9 are here presented. In Fig. 22 is reported the block scheme of the whole control-estimation scheme, built in Simulink environment. The cyan block represents the Kalman filter estimator. Within such block Eq.s from 5.8 to 5.11 are implemented. As reported in the block scheme in Fig. 21, the Estimator takes as input only the measurements available (in the present case the mirrors motion) and the correction coming from the LQI block. As output, the filter gives the estimated state vector $\hat{x}$, which is sent to the feedback path to close the control loop.
Both process and measurements are affected by noise. Such disturbance has been modeled through the block *Random Number*, which generates normally distributed random signals, with a specific variance defined by the user.

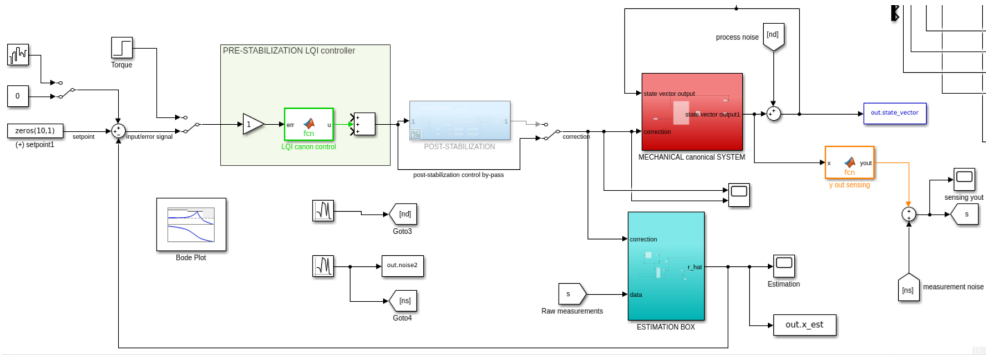

Figure 22: Simulink block scheme of the LQIG control and Kalman filter implementation.

In Fig. 23 are plotted the acquired raw measurements of the mirrors displacements. Both signals are affected by noise. These two signals compose the sensing vector y to be filtered.

In Fig. 24, instead, is reported noisy state vector, as representation of the disturbance affecting the process.

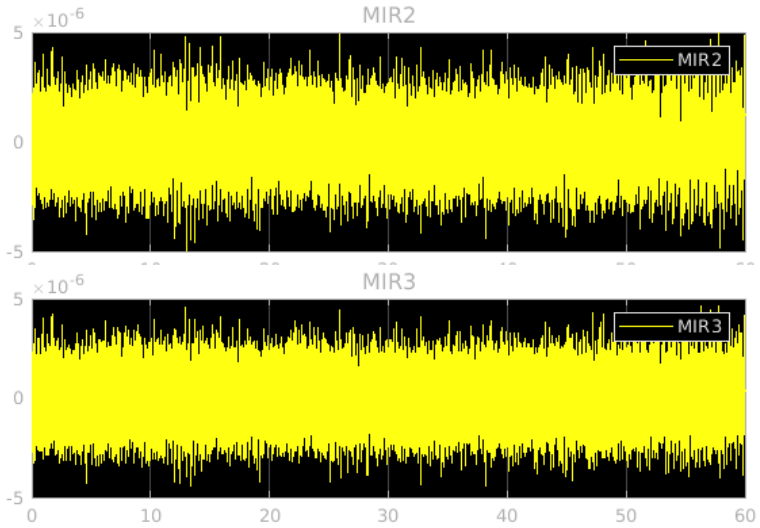

Figure 23: Raw measurements polluted by noise: sensing vector containing mirrors motion

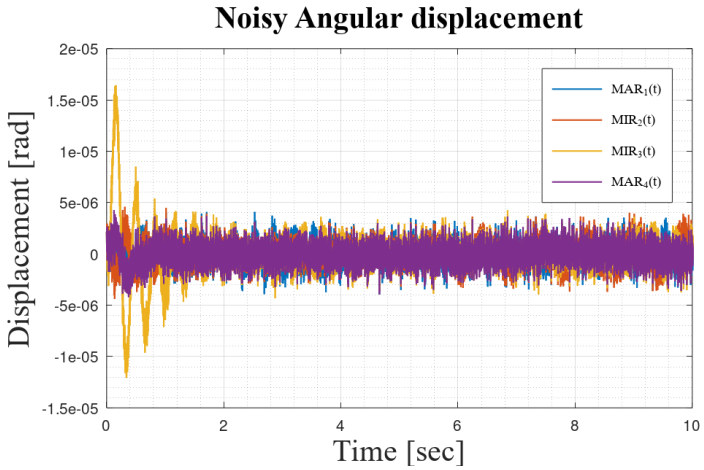

Figure 24: State vector affected by process noise.

The Kalman fitler implemented is able to extract the estimation of the motion of the mirrors, together with the other state variables in order to create the vector $\hat{x}$ to close the control loop.
Such estimations are reported in Fig.s 25, 26 and 27, respectively.

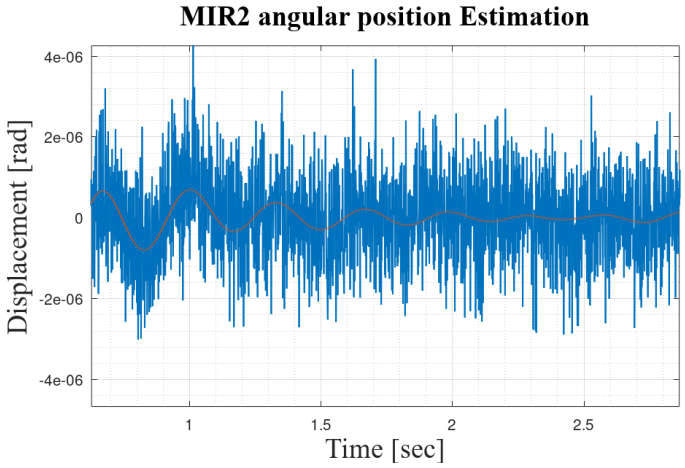

Figure 25: Estimation of the Input mirror motion: in blue is reported the raw measurement affected by noise, while in red the superposed estimation performed by the Kalman filter.

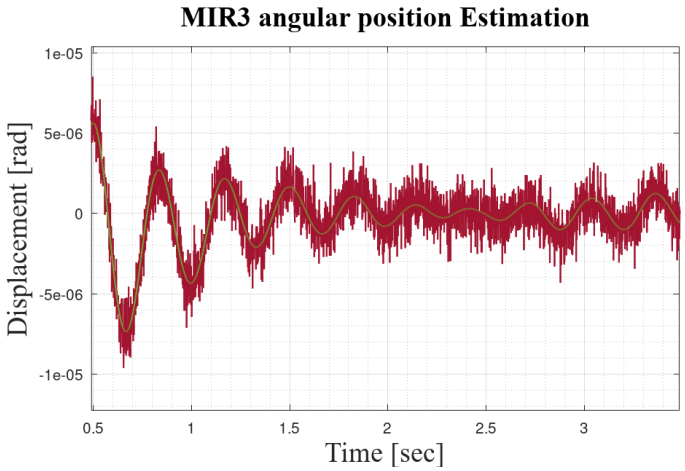

Figure 26: Estimation of the End mirror motion: in red is reported the raw measurement affected by noise, while in green the superposed estimation performed by the Kalman filter.

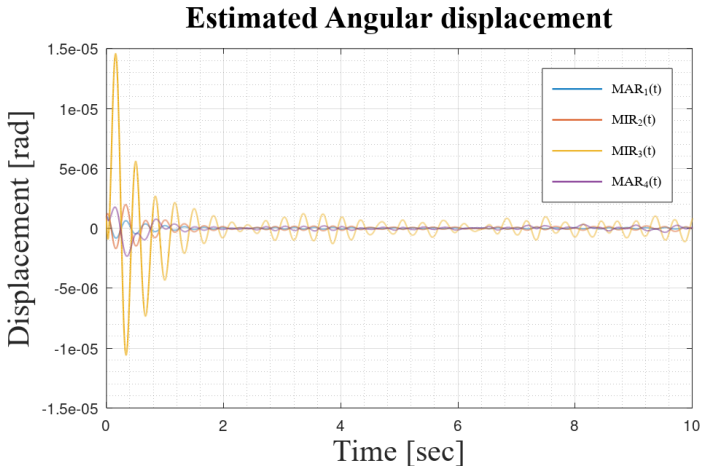

Figure 27: Estimation of the state vector $\hat{x}$. In the plot are reported only the estimated motion of the four masses.

In the last plot (Fig. 27, the state vector estimation) only the estimated motion of the four masses are displayed. Together with the estimated velocities, the feedback loop is closed.
As shown the behaviour of the displacement is similar to the one predicted by the ideal simulations with no Kalman filter implemented, see Fig. 15.
The only difference is related to a residual oscillation present in all the displacement signals, especially the one of the End mirror MIR_3. Such behaviour is probably due to the use of a modeled sensors noise too high in terms of amplitude. With such conditions, the filter is anyway able to converge to a steady-state solution, but the presence of the high noise is affecting the results as the system seems to oscillate around the setpoint.

6 Concluding remarks

In the present document, a new strategy for the angular control of an asymmetric opto-mechanical system, i.e. AdV+ Phase II configuration, has been proposed.
The whole control architecture starts from the analytical description of the full-payload (bottom stage) which allows to obtain a State Space modeling of the system.
However, given the asymmetric mechanical configuration of the investigated system (large terminal masses), some problems arise during the diagonalization process: indeed, considering the full-system, it is not possible to fully decouple the different degrees of freedom (modes of vibration). This difficulty is translated in an impossibility to use SISO-like control strategies.
For this reason, the possibility to study the full-coupled system, so to design MIMO-like controllers, is investigated instead.

The State Space formalism plays an important role in this study, as its mathematical architecture handles well the manipulation of MIMO system, and allows as well the possibility to exploit Optimal Control techniques to design advanced controller for the specific system.

The design of an optimal LQR (Linear Quadratic Regulator) controller with an additional integral term (i.e. LQI) has been performed.
Such control is based on the minimization of a specific cost function (built taking into account the state convergence and the control effort requirements) which allows to obtain direct closed-loop stability. By choosing the Canonical representation of the system, we are able to control all the unstable resonances of the plant, by setting the bandwidth of the loop beyond the last unstable pole with a UGF at 5 Hz and a Phase-margin higher than 68 deg.

However, one limitation arises since in real working conditions we want ideally to reduce the noise re-introduction as much as possible above 10 Hz. To fulfill such requirements, dedicated structures such as Roll-off filters (e.g. Low-pass, Elliptic filters...) need to be used. The use of such structures will cause a consistent loss of the Phase-margin available that, in case we want to make sure to control the high resonance mode (i.e. 3 Hz), will lead to a very restricted range of stability margin. One solution will be to put the UGF of the loop before the 3 Hz mode, that is to reduce the bandwidth of the loop and so to left out the possibility to be able to control such mode.

This whole control technique is however based on the hypothesis that we can observe all the variables composing the state vector, while in real working conditions this is not the case. Indeed, we don't usually have information regarding the velocities and other physical quantities; additionally, all the acquired measurements are affected by external disturbances such as sensor noise and process noise.
This issue is solved by the implementation of a state estimator, which is the Kalman Filter.

Through an optimal blending between the model describing the system and the available raw measurements, such filter is able to perform an estimation of the whole variables composing the state vector deprived by noise. The estimation is an optimal process performed through the minimization of the error between the theoretical model and the estimated process. The output of the filter is used as feedback branch of the global control loop architecture, the LQIG estimator (Linear Quadratic Integral Gaussian estimator).

Results of the implemented strategy, although preliminary, showed the potential of the proposed control technique.

Further analysis will foresee the use of the same strategy to design controller for the Pitch degree of freedom, that is TX (already on-going).
Once proper controllers for all the interesting DoFs are ultimately designed, dedicated simulations with the full-ITF model will be performed (Finesse).
In parallel, an update on the Simulink model is on-going, that is to improve the possibility to perform real working conditions studies, by increasing the number of coupling between the different DoFs, like the longitudinal-to-angular.

References

[1] Frank L. Lewis "Applied Optimal Control and Estimation - Digital Design and Implementation" - Prentice Hall and Digital Signal Processing Series, Texas Instruments, 1992.

[2] John A. Sidles "Optical Torques in Suspended Fabry-Perot Interferometers" - LIGO-P030055-C, Physical Letters A, 2006.

[3] Aldo Sestieri "Dispense del corso di MECCANICA DELLE VIBRAZIONI" - Universita' di Roma La Sapienza Dip. di Ingegneria Meccanica e Aeronautica, 2010.

[4] M. Boldrini, J. Casanueva, M. Mantovani and E. Majorana "Analytical Diagonalization of the Driving Matrix for a Fabry-Perot Cavity" - VIR-0211A-20.

[5] Sigur Skogestad, Ian Postlethwaite "Multivariable Feedback Control: Analysis and Design" - Wiley Interscience, Second Edition, 2005.

[6] Antonio Carcaterra "Vehicle systems dynamics and mechatronics" - Sapienza Universita' di Roma, Department of Mechanical and Aerospace Engineering, 2018.
2, 11

3

6

6

11

24